IRAQI JOURNAL OF MATERIALS
Volume (4) Issue (2) April-June 2025, pp. 75-80

Laser-Synthesized Graphene-Supported Platinum-Based Catalysts Used for Electrochemical Energy Storage

Elmunsef Alfasi, Teroch Lazraoui

Department of Chemistry, Faculty of Science, Sidi Mohamed Ben Abdellah University, Fez City, MOROCCO

Abstract
In this work, using epitaxial graphene as a supporting material for the platinum-based catalysts used for electrochemical energy storage is presented. The epitaxy of graphene support layer was carried out by UV laser irradiation of graphene buffer layer on silicon carbide surface. Results showed that when platinum coverage increases, the available graphene surface area decreases, and the growth mechanism shifts toward nucleation on existing clusters. As well, the desorption spectra of deuterium on platinum clusters on graphene exhibit a peak at around 185°C, followed by a broad shoulder with an increasing signal. As platinum coverage increases, the peak at 185°C becomes more pronounced.

Keywords: Graphene; Platinum-based catalysts; Electrochemical energy storage; Support materials
Received: 15 January 2025; **Revised:** 11 March 2025; **Accepted:** 25 March 2025; **Published:** 1 April 2025

1. Introduction

Energy storage plays a critical role in modern energy systems, enabling the efficient use of renewable resources like solar and wind [1]. By capturing energy when production exceeds demand and releasing it when needed, storage systems help stabilize power grids and enhance reliability [2]. Technologies like batteries, pumped hydro, and thermal storage are widely used, with lithium-ion batteries being the most prominent due to their high energy density and efficiency [3,4]. Emerging innovations, including solid-state batteries and hydrogen storage, promise to further transform the sector [5]. As energy demands grow and the shift toward renewable sources accelerates, energy storage will remain essential for a sustainable future [6].

Electrochemical energy storage plays a crucial role in modern energy systems, offering efficient and sustainable solutions for storing and utilizing energy [7]. It involves the conversion of electrical energy into chemical energy, which can be stored and later converted back to electricity when needed [8]. Common technologies include batteries (e.g., lithium-ion, sodium-ion), supercapacitors, and fuel cells [9-11]. These systems are integral to renewable energy integration, electric vehicles, and portable devices, addressing the intermittent nature of solar and wind power [12,13]. Advances in materials science, such as improved electrodes and electrolytes, aim to enhance energy density, efficiency, and cycle life, driving the evolution of clean energy solutions [14-16].

Catalysts play a crucial role in energy storage applications by enhancing the efficiency and sustainability of key chemical reactions. In electrochemical systems like fuel cells and batteries, catalysts accelerate reactions such as oxygen reduction and hydrogen evolution, reducing energy losses and improving overall performance. Platinum-based catalysts, for example, are widely used due to their high activity and stability [17-19]. By lowering activation energy, catalysts enable faster reaction rates at lower temperatures, making energy storage systems more efficient and cost-effective. Furthermore, advancements in catalyst design, such as developing durable and cost-efficient materials, are pivotal for advancing renewable energy technologies and enabling a cleaner energy future [20-25].

Platinum-based catalysts play a critical role in energy storage technologies, particularly in fuel cells and metal-air batteries [26]. Renowned for their exceptional catalytic activity and stability, platinum catalysts efficiently facilitate the oxygen reduction reaction (ORR), a key process in electrochemical energy conversion [27]. However, their high cost and scarcity pose challenges, prompting research into advanced support materials that enhance performance and durability while reducing platinum usage [28]. Innovations like carbon-based supports, metal oxides, and nanostructured materials improve

catalytic activity, stability, and resistance to degradation [29-32]. These advancements make platinum-based catalysts more efficient and cost-effective, contributing significantly to the development of sustainable energy storage systems [33-35].

The enhancement of platinum (Pt)-based catalysts through advanced support materials has revolutionized their performance in electrochemical applications, particularly in oxygen reduction reactions (ORRs) [36,37]. Support materials, such as carbon-based structures, metal oxides, and conductive polymers, play a crucial role in improving the dispersion, stability, and activity of Pt nanoparticles [38,39]. These materials provide high surface area, conductivity, and strong interactions with Pt, reducing aggregation and enhancing catalytic efficiency [40]. Additionally, some supports introduce synergistic effects, boosting ORR kinetics and durability [41]. Innovations in nanostructured and hybrid supports are paving the way for more cost-effective and sustainable Pt-based catalysts, vital for energy storage and fuel cell technologies [42-44].

Graphene has emerged as an excellent support material for platinum (Pt)-based catalysts, particularly in oxygen reduction reactions (ORR) for electrochemical energy storage applications [45]. Its exceptional properties, including high surface area, outstanding electrical conductivity, and robust mechanical strength, enhance catalyst dispersion and electron transfer [46,47]. Graphene's two-dimensional structure enables uniform Pt nanoparticle distribution, reducing agglomeration and maximizing active sites for ORR [48]. Moreover, its chemical stability and resistance to corrosion extend catalyst durability, addressing challenges faced by traditional carbon supports [49]. Functionalization of graphene further improves Pt interaction, optimizing catalytic performance [50]. As a result, graphene-supported Pt catalysts show significant potential in advancing fuel cells and batteries [51].

In this work, using graphene as a supporting material for the platinum-based catalysts used for electrochemical energy storage is presented. The graphene support layer was synthesized by UV laser irradiation of graphene buffer layer on silicon carbide surface.

2. Experiment

Epitaxial graphene samples were prepared through thermal decomposition on silicon carbide (SiC) in a custom experimental furnace. Graphene growth occurred on the silicon face of 4H–SiC(0001), using a graphite crucible placed in a vacuum environment (10^{-6} mbar) and heated to 1500°C for 10 minutes. This process produced graphene surfaces consisting of a mixture of monolayer and bilayer graphene, with monolayer coverage exceeding 70%. The graphene's quality, composition, uniformity, and thickness were initially assessed using atomic force microscopy and Raman spectroscopy. As shown in Fig. (1), before platinum deposition, the graphene samples were irradiated with UV laser pulses (~1 J/cm^2 fluence) to perform rapid annealing, followed by 20 minutes thermal annealing at 700°C to remove contaminants and ensure clean surfaces. Temperatures were monitored using a thermocouple in direct contact with the sample holder, cross-verified with a pyrometer. The high quality of the graphene films was confirmed by atomically resolved scanning tunneling microscopy (STM) images.

Platinum was deposited onto graphene at room temperature using an electron-beam evaporator, with STM imaging used to calibrate Pt coverage. Hydrogenation of Pt clusters for thermal desorption spectroscopy (TDS) was performed by exposing the samples to molecular deuterium at 10^{-5} mbar and 27°C for 10 minutes. Deuterium, being chemically identical to hydrogen but less abundant in the vacuum chamber, provided a better signal-to-noise ratio for TDS. During TDS measurements, samples were placed in front of a mass spectrometer, heated at a constant rate of ~15°C/s to target temperatures (400–750°C), and monitored via the mass 4 channel.

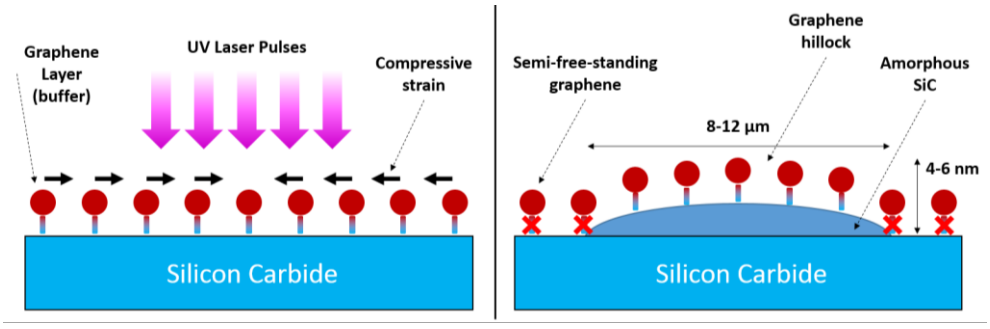

Fig. (1) Scheme of the experimental system used in this work

3. Results and Discussion

The Pt growth on graphene was analyzed and figure (2) shows the amount of graphene surface area covered by Pt clusters with respect to the total area scanned (Pt area coverage) versus the total volume of the Pt clusters, upon room temperature Pt deposition at constant flux.

From STM imaging at the atomic level, the Pt atoms result to be arranged with (111) packing. Thus, we define 1 monolayer (ML) as the Pt atom density in Pt(111). A lattice constant of 0.383 nm yields 1 ML = 1.61×10^{15} atoms/cm^2. Whereas the interlayer distance is about 0.221 nm. Figure (3) shows STM images of the epitaxial graphene surface with 0.62 ML, 1.48 ML, and 4.5 ML of Pt. These scans are representative of the surface morphology in the Pt growth regimes that we identified and which will be discussed in the following.

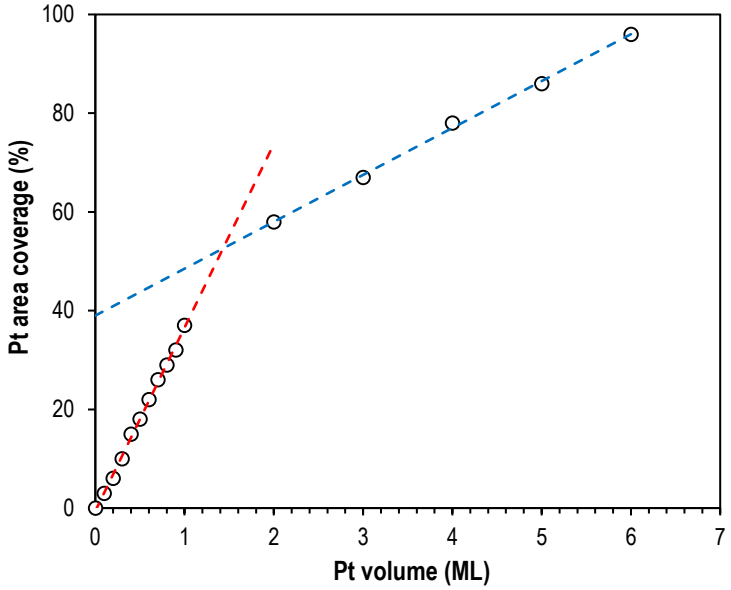

Fig. (2) Area coverage (%) versus the total cluster volume (ML)

At Pt coverages up to approximately 1 monolayer (ML), platinum particles tend to disperse randomly across the graphene surface. As the Pt coverage increases, the cluster density rises from only a few clusters, each containing at least 5-10 Pt atoms, to around 176 clusters per 100x100 nm². However, the average height of the clusters remains largely consistent. A typical surface morphology for this coverage is depicted in Fig. (3a), representing a surface with 0.62 ML of Pt, covering 28% of the graphene area. The Pt clusters range in diameter from 1.5 nm to 11.5 nm, with an average diameter of about 6.5 nm, and their height varies from 0.5 nm to 2.5 nm, averaging around 0.8 nm. In this growth regime, a linear relationship is observed between the volume of Pt and the area coverage, with the intercept being zero.

When Pt coverage exceeds 3 ML, the clusters begin to merge, and as a result of coalescence, their density drops from around 38 clusters to a single cluster per 100x100 nm² at full coverage. Meanwhile, the average height of the clusters increases significantly. At a Pt coverage of 4.5 ML, corresponding to 95% area coverage (as shown in Fig. 3c), the average height rises to 2 nm, with the maximum height reaching 5.4 nm. Even in this regime, a linear relationship between Pt volume and area coverage is observed, although with a smaller slope and an intercept around 51% area coverage. As the Pt volume increases, the curve approaches 100% area coverage asymptotically.

The two growth regimes can be better understood by considering the interaction strength between Pt and the graphene substrate compared to the cohesive energy of Pt–Pt interactions. It is worth noting that no Pt intercalation occurred during deposition at room temperature. At low coverage, the cluster growth is mainly influenced by the balance between adsorption and desorption on the graphene surface. If all the evaporated Pt atoms were to stick to the graphene and follow a layer-by-layer growth mechanism, saturation would occur at 1 ML coverage. However, the linear fit for the first growth phase shows full coverage at about 1.85 ML, suggesting that in the early growth stages, the average cluster height is nearly 2 layers, which aligns with the measured value of 0.6 nm. As coverage increases, the available graphene surface area decreases, and the growth mechanism shifts toward nucleation on existing clusters. Additionally, since the evaporator flux remains constant, the non-zero intercept from

the linear fit of the second growth phase indicates that the Pt–graphene interaction is weaker than Pt–Pt interactions. This explanation is consistent with the data presented in Fig. (2).

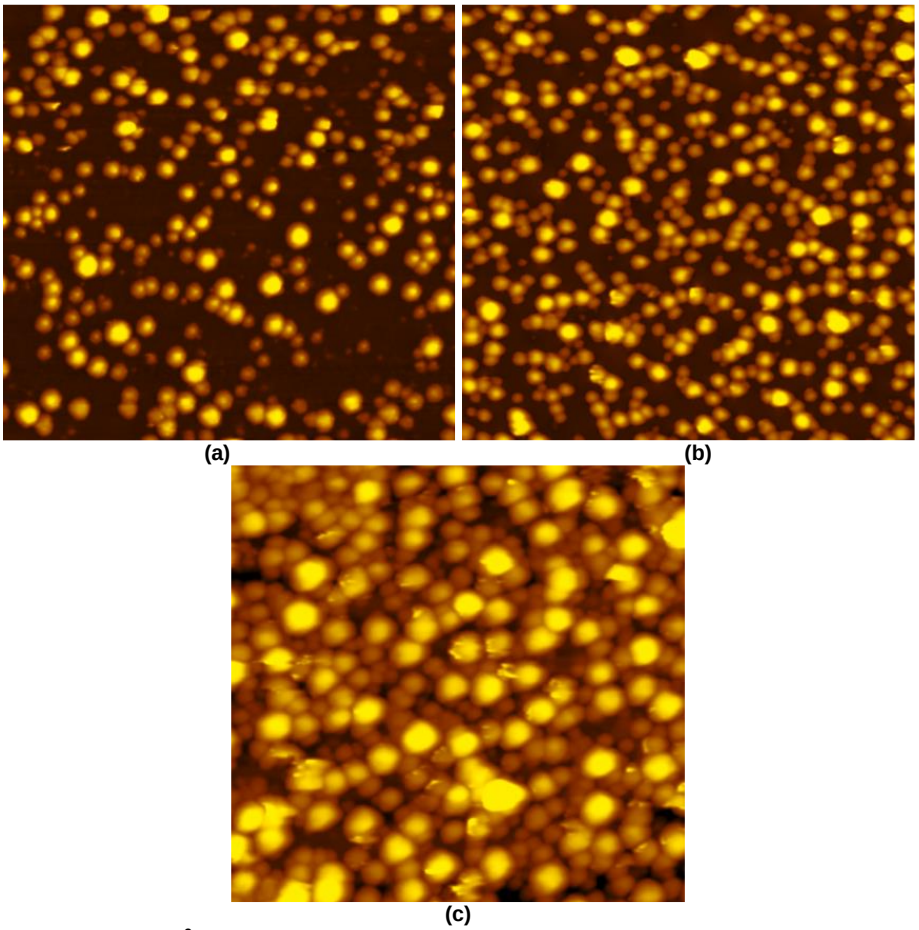

Fig. (3) STM scans of 100x100nm^2 areas representative of the surface with a Pt content (a) 0.62 ML – 28% (green), (b) 1.48 ML – 51% (blue), and (c) 4.5 ML – 95% (red). Colors for the frames of STM images (a)–(c) have been used accordingly to the colors of the data points highlighted in Fig. (2)

The adsorption of deuterium (D_2) on Pt-covered graphene was investigated and analyzed with increasing Pt content. For this purpose, more Pt was gradually deposited onto the sample. After each deposition, the sample was exposed to molecular hydrogen (D_2) and TDS was performed. The sample was heated to 450°C, at which, the Pt island shape as well as the distribution remained mostly unchanged, as revealed by the STM results. Higher temperatures may cause a significant, irreversible morphological changes, so the 450°C was the highest limit of temperature for TDS measurements. Figure (4) shows the temperature-dependent D_2 desorption behaviors for various Pt coverages. Pure graphene (0% Pt) exposed to D_2 displayed minimal adsorption, which agrees with the fact that D_2 does not adsorb onto defect-free graphene at room temperature. The D_2 desorption spectra of Pt clusters on graphene, shown in Fig. (4), exhibit a peak around 185°C, followed by a broad shoulder with an increasing signal. As Pt coverage increases, the peak at 185°C becomes more pronounced.

4. Conclusion

In concluding remarks, using epitaxial graphene as a supporting material for the platinum-based catalysts used for electrochemical energy storage is presented. The epitaxy of graphene support layer was carried out by UV laser irradiation of graphene buffer layer on silicon carbide surface. Results showed that when platinum coverage increases, the available graphene surface area decreases, and the growth mechanism shifts toward nucleation on existing clusters. As well, the desorption spectra of deuterium on platinum clusters on graphene exhibit a peak at around 185°C, followed by a broad shoulder with an increasing signal. As platinum coverage increases, the peak at 185°C becomes more pronounced.

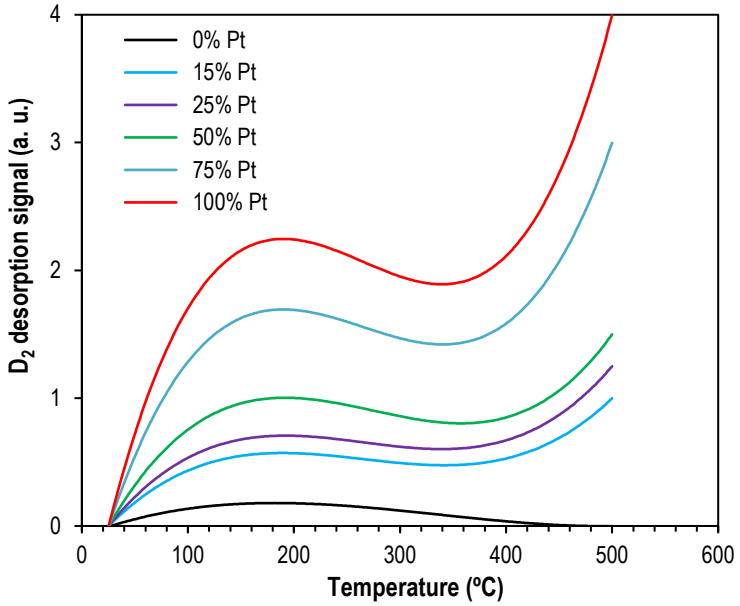

Fig. (4) TDS spectra of D_2 desorption from Pt clusters supported on graphene. Pt coverage ranging from 0 to 5 ML.

References

[1] H. Yuan, H. Chen, D. Li, L. Deng, J. Chen, Y. Fan, M. He, and F. Sun, Electrochem. Commun., 100 (2019) 52-59.
[2] M. Lim, J.Y. Kim, H. Kang, T.W. Yun, H.-B. Cho, and Y.-H. Choa, Sens. Actuat. Rep., 8 (2024) 100247.
[3] C.P. Keshavananda Prabhu, K.R. Naveen, and J. Hur, RSC Appl. Interfaces, 1(2) (2024) 301-312.
[4] K. Baruah and P. Deb, Nanoscale Adv., 3(13) (2021) 3681-3707.
[5] S.J. Martínez, A. Lavacchi, E. Berreti, L. Capozzoli, C. Evangelisti, A. Arranz, J.L. Rodríguez, and E. Pastor, Inorganica Chimica Acta, 566 (2024) 122008.
[6] S. Jia, M. Hong, H. Xiao, X. Liu, and X. Tong, Carbon Trends, 16 (2024) 100374.
[7] J. Cai, J. Chen, Y. Chen, J. Zhang, and S. Zhang, iScience, 26(5) (2023) 106730.
[8] S.J. Gutic, M. Šabanović, D. Metarapi, I.A. Pašti, F. Korać, and S.V. Mentus, Int. J. Electrochem. Sci., 14(9) (2019) 8532-8543.
[9] A. Vulcu, T. Radu, A. Turza, and C. Berghian-Grosan, Appl. Surf. Sci. Adv., 21 (2024) 100609.
[10] J. Li, W.-Y. Zan, H. Kang, Z. Dong, X. Zhang, Y. Lin, Y.-W. Mu, F. Zhang, X.-M. Zhang, and J. Gu, Appl. Catal. B: Enviro., 298 (2021) 120510.
[11] N. Khossossi and P. Dey, J. Energy Chem., 100 (2025) 665-673.
[12] H. Ma, Y. Tong, Y.M. Hung, and X. Wang, Process Safety Enviro. Protect., 192 (2024) 358-377.
[13] I.Y. Khairani, B. Jin, S.M. Palardonio, U. Hagemann, B. Alonso, A. Ortega, C. Doñate-Buendía, J. Martorell, C. Ros, T. Kallio, and B. Gökce, J. Catal., 439 (2024) 115771.
[14] Y. Huang, D. Wang, Y. Wei, X. Dong, R. Yang, H. Li, M. Wei, J. Yu, L. Zhong, and Y. Xu, Arabian J. Chem., 17(2) (2024) 105533.
[15] S. Dhali, M. Karakoti, G. Tatrari, S. Pandey, K.S. Rawat, C. Tewari, B.S. Bhushan, Y.C. Jung, A. Srivastava, and N.G. Sahoo, Mater. Adv., 5(9) (2024) 3771-3782.
[16] S. Rowshanzamir, M. Jafari, N. Nozarian, M.J.Parnian, Results in Chem., 7 (2024) 101383.
[17] Z. Liu, X. Hu, X. Dong, S. Zhao, Y. Chen, B. Zhang, L. Wen, and L. Wang, Cell Reports Phys. Sci., 4(2) (2023) 101256.
[18] S. Calabuig-Mompó, D. Cazorla-Amorós, and E. Morallón, J. Electroanal. Chem., 955 (2024) 118069.
[19] K. Cysewska, M. Łapiński, M. Zając, J. Karczewski, P. Jasiński, and S. Molin, Beilstein J. Nanotechnol., 14 (2023) 420-433.
[20] A. Mollar-Cuni, S. Martín, G. Guisado-Barrios, and J.A. Mata, Carbon, 206 (2023) 314-324.
[21] A. Manimozhi, T. Sumathi, Sreeja Saravanan, N. Dhachanamoorthi, M. Saravanakumar, and K. Jayaprakash, Chem. Phys. Impact, 10 (2025) 100779.
[22] X. Zeng, S.K. Mitra, and X. Li, Int. J. Hydrogen Energy, 86 (2024) 577-585.
[23] L.M. Mohlala, T.-C. Jen, and P.A. Olubambi, Procedia Manufact., 35 (2019) 1250-1255.
[24] X. Chen, K. Niu, Z. Xue, X. Liu, B. Liu, B. Zhang, H. Zeng, W. Lv, Y. Zhang, and Y. Wu, Nanoscale Adv., 4(6) (2022) 1639-1648.
[25] S. Rodriguez-Miguel, Y. Ma, G. Farid, R. Amade, R. Ospina, J.L. Andujar, E. Bertran-Serra, and S. Chaitoglou, Heliyon, 10(10) (2024) e31230.
[26] J. Chen, M. Perez-Page, C.M.A. Parlett, Z. Guo, X. Yang, Z. Zhou, H. Zhai, S. Bartlett, T.S. Miller, and S.M. Holmes, Chem. Eng. J., 487 (2024) 150670.
[27] A. Yagmur Goren, M. Temiz, D. Erdemir, and I. Dincer, Energy, 315 (2025) 134257.
[28] I. Bardarov, D.Y. Apostolova, P. Martins, I. Angelov, F. Ruiz-Zepeda, I. Jerman, M. Dular, D. Strmcnik, and B. Genorio, Electrochimica Acta, (2025) 145754.
[29] C. Deepa, L. Rajeshkumar, and M. Ramesh, J. Mater. Res. Technol., 19 (2022) 2657-2694.
[30] D. Mladenović, E. Daş, D.M.F. Santos, A.B Yurtcan, Š. Miljanić, and B. Šljukić, J. Alloys Comp., 905 (2022) 164156.
[31] W. Ji, X. Xiao, F. Li, X. Fan, Y. Meng, and M. Fan, RSC Adv., 12(10) (2022) 5797-5806.

[32] Z.A.C. Ramli, J. Pasupuleti, T.S.T. Saharuddin, Y.N. Yusoff, W.N.R. Wan Isahak, L. Baharudin, C.T. Yaw, S.P. Koh, and S.T. Kiong, Alexandria Eng. J., 76 (2023) 701-733.
[33] F.M.B. Gusmão, T. Đurić, J. Milikić, K. Radinović, D.M.F. Santos, D. Stanković, and B. Šljukić, Int. J. Hydrogen Energy, 71 (2024) 763-774.
[34] S.F. Rastegar, R. Pilar, J. Moravkova, G. Sadovska, V.I. Parvulescu, J. Pastvova, J. Plsek, D. Kaucky, N. Kostkova, and P. Sazama, Catal. Sci. Technol., 13(17) (2023) 5120-5130.
[35] A.G. Kamaha Tchekep, V. Suryanarayanan, and D.K. Pattanayak, Carbon Trends, 16 (2024) 100393.
[36] C. Vijina, K.P. Majitha, and S.P. Damodaran, Results in Eng., 20 (2023) 101444.
[37] K. Chida, T. Yoshii, R. Kawaguchi, M. Inoue, F. Tani, T. Sobue, S. Ohtani, K. Kato, T. Ogoshi, S. Nakahata, K. Kamiya, and H. Nishihara, Green Chem., 26(15) (2024) 8758-8767.
[38] M.R. Shaik, M. Al-Othman, M. Kuniyil, A. Al-Warthan, M.R. Hatshan, M.E. Assal, M.N. Tahir, and M. Khan, Arabian J. Chem., 17(4) (2024) 105718.
[39] S. Fajardo, P. Ocón, J.L. Rodríguez, and E. Pastor, Chem. Eng. J., 461 (2023) 142053.
[40] S. Santra, A. Ghosh, B. Das, S. Pal, S. Pal, and A. Adalder, RSC Sustain., 2(6) (2024) 1631-1674.
[41] A. Letona-Elizburu, M. Enterría, A. Aziz, S. Villar-Rodil, J.I. Paredes, J. Carrasco, and N. Ortiz-Vitoriano, Sustain. Mater. Technol., 39 (2024) e00835.
[42] P. Sapkota, S. Lim, and K.-F. Aguey-Zinsou, RSC Sustain., 1(2) (2023) 368-377.
[43] S.R. Ashok Kumar, D. Vasvini Mary, G.A. Suganya Josephine, and M.A. Riswan Ahamed, Hybrid Adv., 5 (2024) 100168.
[44] Y. Balasooriya, P. Samarasekara, C.M. Lim, Y.-F.C. Chau, M.R. Rahimi Kooh, and R. Thotagamuge, Heliyon, 9(5) (2023) e15989.
[45] N. Madima and M. Raphulu, J. Electroanal. Chem., 976 (2025) 118799.
[46] S.A. Wella, Y. Hamamoto, Suprijadi, Y. Morikawa, and I. Hamada, Nanoscale Adv., 1(3) (2019) 1165-1174.
[47] N.A. Mojapelo, N.S. Seroka, and L. Khotseng, Heliyon, 10(9) (2024) e29907.
[48] Z. Du, F. Yu, J. Wang, J. Li, X. Wang, and A. Qian, RSC Adv., 14(31) (2024) 22486-22496.
[49] A. Zamljen, Ž. Lavrič, A. Prašnikar, J. Teržan, M. Grilc, A. Meden, and B. Likozar, Renew. Energy, 226 (2024) 120467.
[50] A. Magaji, D.P. Martin, L.-S. Lin, S.A. Krasnikov, A. Kulak, Z. Aslam, R. Drummond-Brydson, and N.N. Sergeeva, J. Photochem. Photobiol. A: Chem., 457 (2024) 115884.
[51] L.E.B. Lucchetti, J.M. de Almeida, and S. Siahrostami, EES Catal., 2(5) (2024) 1037-1058.

 ISSN (print) 2958-8960 (online) 3006-6042 Printed in IRAQ